UDK 669.35'5:620.175:621.777
Professional article/Strokovni članek

ISSN 1580-2949
MTAEC9, 47(4)519(2013)

CONVERSION OF THE Ms70 ALPHA-BRASS TORSION-TEST DATA INTO HOT-FORMING PROCESSING MAPS

PRETVORBA PODATKOV TORZIJSKEGA PREIZKUSA ALFA MEDI Ms70 V PROCESNE ZEMLJEVIDE VROČE PREDELAVE

Tomáš Kubina[1], Josef Bořuta[2], Rudolf Pernis[3]

[1]COMTES FHT, Prumyslova 995, 334 41 Dobrany, Czech Republic
[2]Material & Metallurgical Research Ltd., Pohranicni 693/31, 706 02 Ostrava-Vitkovice, Czech Republic
[3]Faculty of Special Technology, Alexander Dubcek University in Trencin, Trencin, Slovak Republic
tomas.kubina@comtesfht.cz

Prejem rokopisa – received: 2012-09-16; sprejem za objavo – accepted for publication: 2012-12-03

The present paper gives a summary of the plastic behaviour of the Ms70 deep-drawing cartridge brass under the hot-forming conditions explored by using a SETARAM-Vítkovice torsion plastometer. The specimens were cut from the hot-extruded and, subsequently, cold-drawn brass bars.
Formability tests were performed on the diameter 6 mm specimens at (650, 700, 750, 800 and 850) °C and at the speeds of (16, 80, 400 and 800) r/min. These testing conditions are equivalent to the conditions of the ordinary industrial hot extrusion of brass: the single most problematic operation in the manufacturing process in terms of an occurrence of serious defects.
The results of the torsion tests were converted into the conventional format: the maximum flow-stress levels vs. the peak-strain intensity. The points thus obtained can be used for finding the activation energy for forming Q, which is useful for determining the thermally compensated strain rate with the aid of the Zener-Hollomon Z parameter.
The power-dissipation maps with the axes showing the deformation temperature and logarithmic strain rate were computed using a dynamic material model. The calculation of the dissipation efficiency was verified by comparing it with the known data on the 30 % zinc brass. The maps constructed in this manner allow the data from the torsion and compression plastometers to be compared. The paper also includes a discussion of the changes in the processing maps at higher strains showing the optimum regions for the hot extrusion of brass.

Keywords: flow stress, brass, hot formability, strain rate, torsion test, power-dissipation maps

V članku je povzetek plastičnega vedenja globokovlečne medi Ms70 pri vroči predelavi z uporabo torzijskega plastometra SETARAM-Vítkovice. Vzorci so bili izrezani iz vroče iztiskane in nato hladno vlečene palice iz medi.
Preizkusi preoblikovalnosti so bili izvršeni na vzorcih premera 6 mm pri temperaturah (650, 700, 750, 800 in 850) °C in hitrostih (16, 80, 400 in 800) r/min. Te razmere pri preizkusih so enakovredne tistim pri navadnem industrijskem iztiskanju medi; najbolj problematični operaciji pri procesu izdelave zaradi pojava hujših poškodb.
Rezultati torzijskih preizkusov so bili pretvorjeni v navadno obliko: maksimalne natezne napetosti proti največjemu raztezku. Tako dobljene točke se lahko uporabi za izračun aktivacijske energije preoblikovanja Q, ki je uporabna za določanje toplotno kompenzirane hitrosti trganja z uporabo Zener-Hollomon Z-parametra.
Zemljevidi spreminjanja moči z osmi, ki prikazujejo temperaturo deformacije in logaritem hitrosti preoblikovanja, so bili izračunani z dinamičnim modelom materiala. Izračun spreminjanja učinkovitosti je bil preverjen s primerjavo poznanih podatkov za med s 30 % cinka. Tako konstruirani zemljevidi omogočajo primerjavo podatkov iz torzije in plastometra. Članek vključuje tudi razpravo sprememb v zemljevidih procesiranja pri višjih napetostih in prikazuje optimalna področja za vročo ekstruzijo medi.

Ključne besede: napetost tečenja, med, vroča preoblikovalnost, hitrost preoblikovanja, torzijski preizkus, mape spreminjanja moči

1 INTRODUCTION

The Ms70 brass belongs to the group of alpha brasses with deep-drawing properties that are used for making cartridge shells in a cold process. The conventional method of the production of brass cartridge shells uses rolled feedstock. The punching of the blanks from a strip leads to large amounts of waste material that requires reprocessing in metallurgical plants. Munitions plants have launched the projects introducing a zero-waste production of brass cartridge shells from Ms70 bars. This change from the rolled strip feedstock to hot-extruded bars required a technology upgrade in the metallurgical plants.

The hot-extrusion process proved to be the critical stage in the production of brass bars. As the Ms70 brass exhibits excellent cold formability, it is difficult to form it at high temperatures. The flow stress of the Ms70 brass in the extrusion process is governed primarily by the forming temperature, the strain rate and the strain. The most common technique for exploring the flow stress at elevated temperatures is the tension testing.[1,2] However, its results are not adequate for mapping the forming processes at high temperatures and high strain rates. As measuring the flow stress in a production is not cost-effective, the forming process was simulated using a torsion plastometer.[3]

A conversion of the results of the compression plastometer testing into the processing maps for the

30 % zinc brass was reported in[4,5]. The evaluation was based on the dynamic material model reported by Prasad[6]. The total energy absorbed by the deformed body P is converted into two forms: G – causing a rise in the temperature; and J – leading to microstructural changes. The factor that partitions the energy between G and J is the strain-rate coefficient m. There is an effect of the stress as well. The J content can be calculated using the following equation:

$$J = \frac{\sigma \dot{\varepsilon} m}{m+1} \tag{1}$$

where σ is the flow stress and $\dot{\varepsilon}$ denotes the strain rate. An ideal linear dissipator term is given by $m = 1$ and $J = J_{max} = \sigma\dot{\varepsilon} / 2$. The dissipation efficiency for a non-linear dissipator may be expressed as a dimensionless parameter:

$$\eta = \frac{J}{J_{max}} = \frac{2m}{(m+1)} \tag{2}$$

The variation of η with the temperature and strain rate represents a dissipation of the power through the microstructural changes in the workpiece material. The purpose of this study was to compare and contrast the energy-dissipation maps constructed using the data from the compression and torsion plastometers.

2 MATERIALS AND METHODS

The computer that controls the plastometer records the following quantities: time, torque M_k, axial force F, temperature T and the number of twists N. The test specimen for a torsion plastometer is a bar with the diameter of D (radius R) and a gauge length of L. The key output of the torsion test for a formability assessment is the number of twists to fracture N_f. As twisting causes the test bar to shrink in length, the grips are fixed from the beginning of the twisting cycle. Consequently, the axial force F begins to act on the bar. The flow stress is given by the following equation:

$$\sigma = \sqrt{\left(\frac{3\sqrt{3}M_k}{2\pi R^3}\right)^2 + \left(\frac{F}{\pi R^2}\right)^2} \tag{3}$$

The strain intensity e in the torsion testing was found from:

$$e = \frac{2}{\sqrt{3}} \arg\sinh\left(\frac{2\pi RN}{3L}\right) \tag{4}$$

In a hot-torsion test, the stress-strain dependence is monitored under the prescribed conditions (specimen geometry, temperature, strain rate).[7]

The experimental hot-torsion testing was performed using the Ms70 deep-drawing brass with a chemical composition given in **Table 1**. The test specimens were 10 mm diameter bars. Ms70 brass bars were produced in the following sequence: melting in an electric induction furnace, semi-continuous casting of round ingots, hot extrusion and final sizing in a cold-drawing process.

The hot-torsion testing of Ms70 brass bars was performed according to a 4 × 5 schedule. This means that four strain-rate values of (0.2, 1, 5 and 10) s^{-1} corresponding to the twisting speeds of (16, 80, 400 and 800) min^{-1} were combined with five temperature levels of T is (650, 700, 750, 800 and 850) °C.

3 DISCUSSION OF RESULTS

The results of the torsion testing at 650 °C are shown in **Figure 1**. The tests at the other temperatures were evaluated in an identical manner.[8]

The peak stress values σ_p and the corresponding strain levels e_p were derived from these plots. The peak stress (the maximum stress) σ_p is governed by two variables: the temperature and the shear-strain rate. This dependency can be expressed as the function $\sigma_p = f(t, e)$,

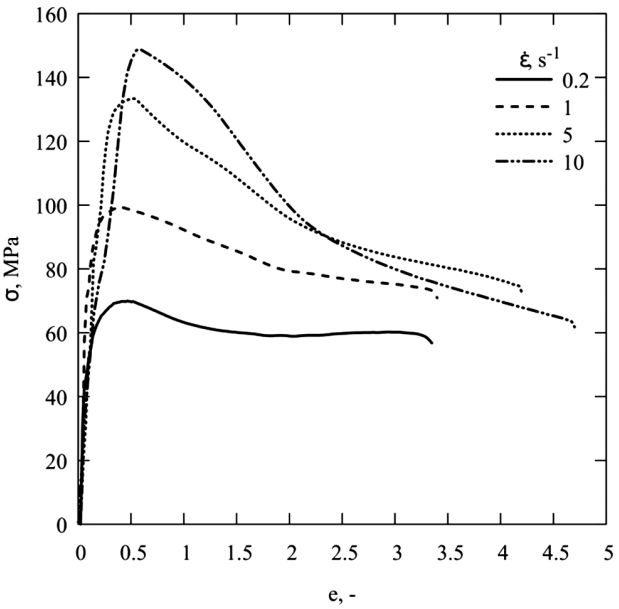

Figure 1: Flow stress of the Ms70 brass at 650 °C
Slika 1: Krivulje tečenja medi Ms70 pri 650 °C

Table 1: Chemical composition of the Ms70 brass for torsion testing
Tabela 1: Kemijska sestava medi Ms70 za torzijske preizkuse

Element	Cu	Pb	Sn	Fe	Ni	Mn	Al	Si
Content, *w*/%	70.39	0.0004	0.0042	0.0232	0.0022	0.0003	0.0012	0.0002
Element	As	Sb	Bi	Cr	Cd	Ag	P	Zn
Content, *w*/%	0.0001	0.0031	0.0001	0.0001	0.0001	0.0001	0.0002	balance

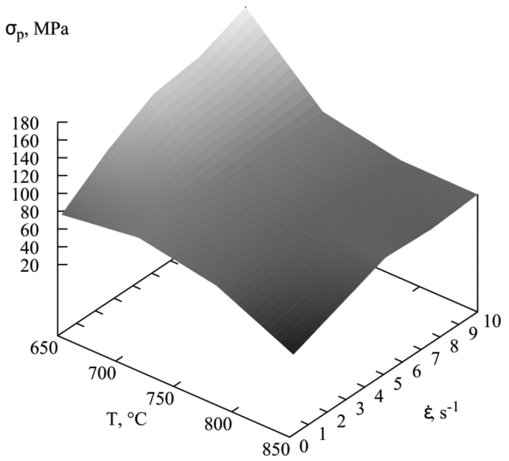

Figure 2: Representation of the $\sigma_p = f(t, e)$ function in a 3D plot
Slika 2: Prikaz funkcije $\sigma_p = f(t, e)$ v 3D-diagramu

which is shown as a 3D-plot in **Figure 2**. This dependence is in line with the expected deformation behaviour of the single-phase materials. The peak flow-stress values decline with the increasing temperature and decreasing strain rate. The $\sigma_p - e$ plots reveal that the Ms70 brass undergoes a recovery during the deformation. The shapes of these curves suggest that a dynamic recrystallization is the primary mechanism. Values σ_p and e_p were used to calculate the activation energy of the deformation and were published in an article.[9]

The ultimate strain e_f (strain to fracture) is another characteristic of a material's formability. The values of the strain to fracture for a torsion testing of the Ms70 brass are summarised in **Figure 3**. The effects of the differences between the strain rates are indistinct but certain trends can be found. Despite the scatter in the measured values resulting from the sensitivity of the torsion test to the inhomogeneity of the test bar surface,

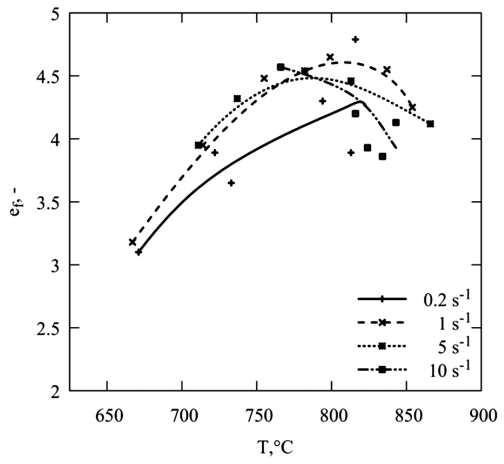

Figure 3: Relationship between the strain intensity to fracture and temperature
Slika 3: Odvisnost med intenziteto napetosti do preloma in temperaturo

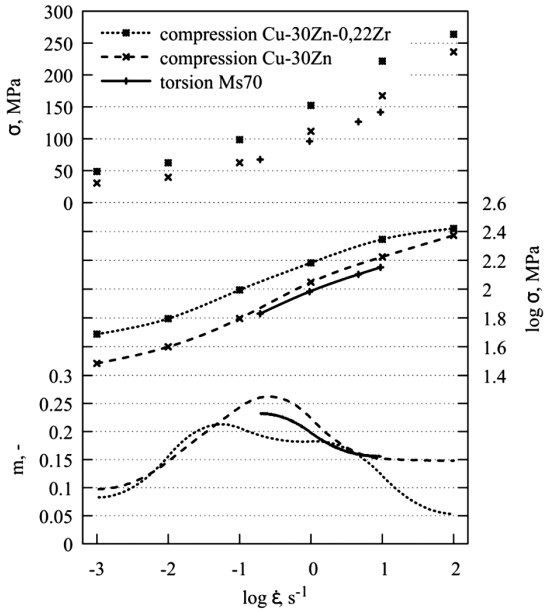

Figure 4: Conversion of the results of the plastometer testing at 650 °C from the recorded stress values at the strain of $e = 0.5$ into the strain-rate coefficient m
Slika 4: Pretvorba rezultatov preizkusov na plastometru pri 650 °C iz zabeleženih vrednosti napetosti pri hitrosti trganja $e = 0,5$ v koeficient hitrosti natezanja m

it is clear that the optimum forming temperature is between 800 °C and 850 °C.

Power-dissipation maps were constructed using the dynamic material model. The power-dissipation coefficient η was found using the following procedure: The stress-strain rate function was transformed into the log-stress vs. log-strain rate relationship (**Figure 4**).

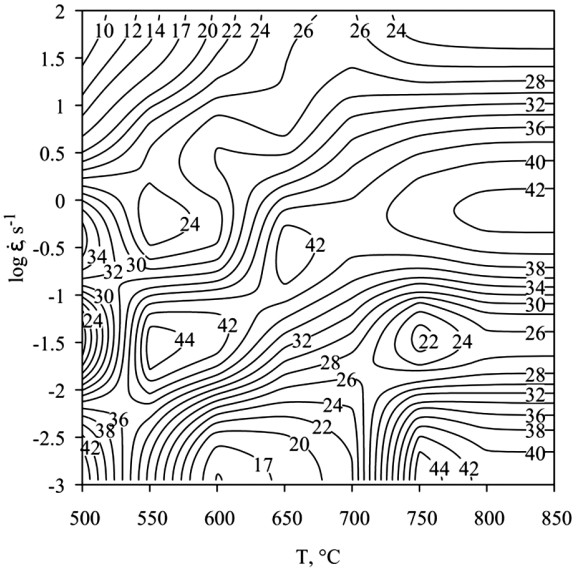

Figure 5: Power-dissipation map for the alpha brass with 30 % Zn constructed from the data from[10] for the strain of 0.5. The numbers represent dissipation efficiency in fractions (%).
Slika 5: Zemljevid raztrosa moči za alfa med s 30 % Zn, konstruiran iz podatkov iz[10] za hitrost trganja 0,5. Številke pomenijo učinkovitost raztrosa v deležih (%).

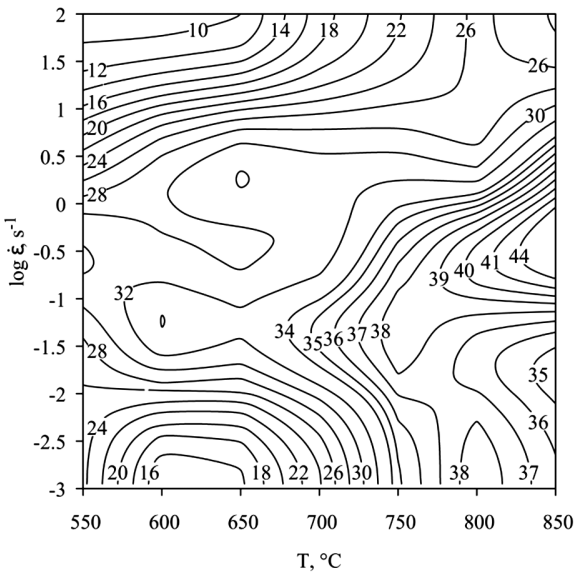

Figure 6: Power-dissipation map for the alpha brass with 30 % Zn and 0.20 % Zr constructed from the data from[5] for the strain of 0.5. The numbers represent dissipation efficiency in fractions (%).

Slika 6: Zemljevid raztrosa moči za alfa med s 30 % Zn in 0,20 % Zr, konstruiran iz podatkov iz[5] za hitrost trganja 0,5. Številke pomenijo učinkovitost raztrosa v deležih (%).

Cubic splines were used to find the log-stress values between the experimentally measured points, from which the strain-rate coefficient was calculated. **Figure 4** illustrates three different dependences at the temperature of 650 °C. The stress curve from the torsion plastometer

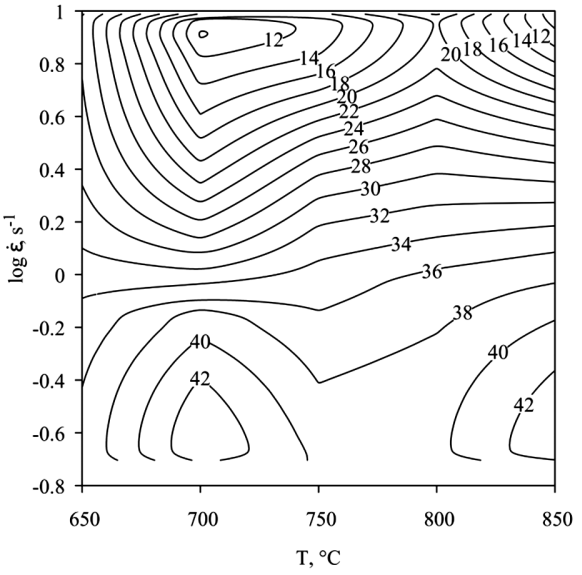

Figure 7: Power-dissipation map for the alpha brass with a chemical composition according to **Table 1** constructed from the data measured with the SETARAM-VÍTKOVICE torsion plastometer for the strain rate of 0.5. The numbers represent dissipation efficiency in fractions (%).

Slika 7: Zemljevid raztrosa moči za alfa med s kemično sestavo iz **tabele 1**, konstruiran iz podatkov, izmerjenih s torzijskim plastometrom SETARAM- VÍTKOVICE , za hitrost trganja 0,5. Številke pomenijo učinkovitost raztrosa v deležih (%).

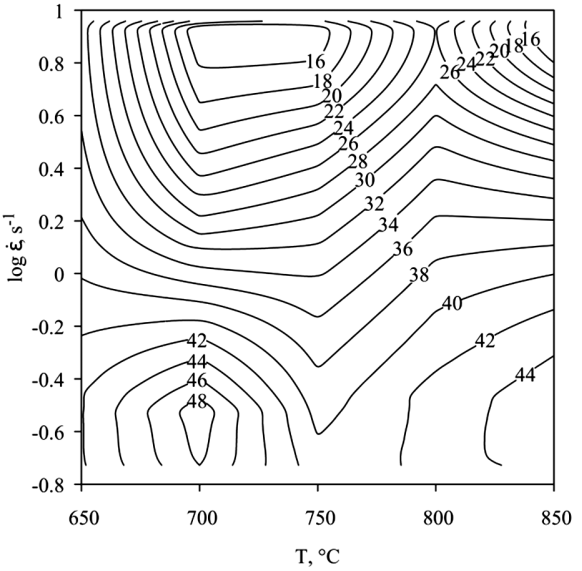

Figure 8: Power-dissipation map for the alpha brass with a chemical composition according to **Table 1** constructed from the data measured with the SETARAM-VÍTKOVICE torsion plastometer for the strain rate of 0.9. The numbers represent dissipation efficiency in fractions (%).

Slika 8: Zemljevid raztrosa moči za alfa med s kemično sestavo iz **tabele 1**, konstruiran iz podatkov izmerjenih s torzijskim plastometrom SETARAM- VÍTKOVICE, za hitrost trganja 0,9. Številke pomenijo učinkovitost raztrosa v deležih (%).

has a narrow range of strain rates. The other curves are based on the values for the 30 % Zn brass published in[10] and the values for the brass with the mass fraction of Zn 30 % and 0.22 % Zr reported in[5]. The strain-rate coefficient *m* vs. the log-strain-rate relationship is very similar in all the CuZn30 brasses, regardless of the testing-machine type. The peak value of the m coefficient is lower in the brass with a 0.22 % Zr addition.

Figure 5 shows the power-dissipation map for the 0.5 strain in the brass with 30 % zinc. This map was developed using the values published in[10]. Upon the comparison with the map shown in[10], certain differences become apparent, such as that between the high temperature and low-strain rate areas. In the original map, dissipation increases in this area. In the map constructed upon a re-calculation, a region with a decrease followed by an increase is found. The maps re-calculated for the brass with 30 % zinc and 0.22 % Zr do not exhibit any substantial differences (**Figure 6**). Their characters are very similar but the absolute values are shifted. This may be attributed to the algorithm used for constructing the 3D map. The new procedure obviates excessive smoothing of dissipation-coefficient curves at the individual temperature levels. The older maps were constructed to verify the entire procedure: to allow a comparison with the power-dissipation map for the 0.5 strain obtained from the torsion test.

As evidenced by **Figure 7**, the ranges of the strain rates and temperatures are narrower than in the studies reported in[5,10]. The SETARAM torsion plastometer

cannot cover the range of high strain rates due to the physical limitations of the torsion testing. The lower strain rates are achievable with the use of an additional gearbox. However, they were not explored as the original experiment was aimed at the dynamic recrystallization as the governing recovery process. A comparison with the re-calculated power-dissipation maps in **Figures 5** and **6** shows a good agreement with the shape for the brass with 30 % zinc (**Figure 5**). However, substantial deviations can be found at the points representing the limit strain rates, as the procedure for finding the m values is very sensitive to the algorithm for calculating cubic splines and to the accuracy of the flow-stress values. The strength of the torsion test lies in the use of the large strains, which are not achievable in the compression plastometers. Consequently, the power-dissipation maps were available for the high strains as well, such as that in **Figure 8** for the 0.9 strain. The map documents a high efficiency of the dissipation through the microstructural changes at the lower strain rates for all the deformation temperatures.

4 CONCLUSION

The torsion test allows the temperature and strain-rate dependences of the flow stress to be studied under various deformation conditions. Using the peak stress values found, i.e., the values representing the flow stress, the extrusion force can be calculated and the examples for Ms70 are published in[11]. The torsion simulation over a wide range of deformation temperatures suggested that the capacity of the Ms70 brass for deformation may become depleted. A technological testing of hot extrusion[12,13] showed that the formability of brass is poor, which leads to transverse surface cracking. The results of the torsion plastometer testing were converted into the power-dissipation maps for selected strain levels. The dissipation-efficiency η values are comparable with the identically processed literature data. However, there are variances resulting from the difference between the algorithms for computing 3D maps and from the sensitivity to the correct data processing of the boundary strain rates.

Acknowledgment

The results presented in this paper were obtained within the project West-Bohemian Centre of Materials and Metallurgy CZ.1.05/2.1.00/03.0077, co-funded by the European Regional Development Fund.

5 REFERENCES

[1] M. Buršák, J. Bacsó, Skúšanie, kontrola a hodnotenie kvality materiálov, Emilena, Košice 2008

[2] R. Pernis, O. Híreš, J. Kasala, Rozdelenie mechanických vlastností ťahanej mosadznej tyče po priereze, In: Metal 2009, 18th international material and metallurgical conferences, Hradec nad Moravicí, ČR [CD-ROM], Ostrava, Tanger, 2009, 8

[3] I. Schindler, J. Bořuta, Utilization Potentialities of the Torsion Plastometer, Silesian Technical University, Katowice, 1998, 104

[4] D. Padmavardhani, Y. Prasad, Effect of zinc content on the processing map for hot-working of alpha-brass, Materials science and engineering A, 157 (**1992**) 1, 43–51

[5] D. Padmavardhani, Y. Prasad, Effect Of Zirconium On The Processing Maps For Hot-working Of Alpha And Alpha-beta Brass, Zeitschrift Fur Metallkunde, 84 (**1993**) 1, 57–62

[6] Y. Prasad et al., Modeling of dynamic material behavior in hot deformation: Forging of Ti-6242, Metallurgical and Materials Transactions A, 15 (**1984**), 1883–1892

[7] J. Bořuta et al., Plastometrický výzkum deformačního chování řízeně tvářených materiálů, Hutnické listy, 61 (**2008**) 1, 80–87

[8] J. Bořuta, T. Kubina, A. Bořuta, Deformační napětí mosazi Ms70 při zkoušce krutem za tepla, Kovárenství, (**2009**) 39, 13–16

[9] R. Pernis, J. Kasala, J. Bořuta, High temperature plastic deformation of CuZn30 brass – calculation of the activation energy, Kovove Materialy, 48 (**2010**) 1, 41–46

[10] D. Padmavardhani, Y. Prasad, Characterization of hot deformation-behavior of brasses using processing maps. 1. alpha-brass, Metallurgical Transactions A, 22 (**1991**) 12, 2985–2992

[11] R. Pernis, J. Bidulská, Nový prístup pri výpočte lisovacej sily z výsledkov krutovej skúšky, Výrobné inžinierstvo, 7 (**2008**) 4, 17–19

[12] J. Kasala, O. Híreš, R. Pernis, Start-up phase modeling of semi continuous casting process of brass billets, In: Metal 2009, 18th international material and metallurgical conferences, Hradec nad Moravicí, ČR [CD-ROM], Ostrava, Tanger, 2009, 6

[13] R. Pernis, O. Híreš, J. Jurenová, Povrchové trhliny pri lisovaní mosadze CuZn30 za tepla, In: Metal 2007, 16th international material and metallurgical conferences, Hradec nad Moravicí, ČR [CD-ROM], Ostrava, Tanger, 2007, 9